Development of Disulfiram-Loaded Poly(Lactic-co-Glycolic Acid) Wafers for the Localised Treatment of Glioblastoma Multiforme: A Comparison of Manufacturing Techniques

IWONA ZEMBKO,[1] IRAM AHMED,[1] ANEESA FAROOQ,[1] JAGDEEP DAIL,[1] PATRICA TAWARI,[2] WEIGUANG WANG,[2] CHRISTOPHER MCCONVILLE[1]

[1]School of Pharmacy, Faculty of Science and Engineering, University of Wolverhampton, Wolverhampton WV1 1LY, UK
[2]Research Institute in Healthcare Science, Faculty of Science and Engineering, University of Wolverhampton, Wolverhampton WV1 1LY, UK

Received 9 July 2014; revised 19 August 2014; accepted 19 November 2014

Published online in Wiley Online Library (wileyonlinelibrary.com). DOI 10.1002/jps.24304

ABSTRACT: Glioblastoma multiforme (GBM) is the most common primary malignant brain tumour in adults with a very poor prognosis. This paper describes the development of disulfiram (DSF)-loaded biodegradable wafers manufactured using three standard techniques: compression, solvent casting and heat compression moulding. The paper demonstrates that neither technique has an adverse effect on the stability of the DSF within the wafers. However, the solvent casting technique results in an interaction between the poly(lactic-co-glycolic acid) (PLGA) and the DSF. The physical state of the DSF within the wafers was dependent on the manufacturing technique, with the DSF in the wafers manufactured by compression or solvent casting retaining between 40% and 98% crystallinity, whereas the DSF in the wafers manufactured using heat compression moulding was completely amorphous. Release of DSF from the wafers is dependent on the degradation of the PLGA, the manufacturing technique used, and the DSF loading. DSF in the compressed and heat compression moulded wafers had a similar cytotoxicity against a GBM cell line compared with the unprocessed DSF control. However, the cytotoxicity of the DSF in the solvent-casted wafers was significantly lower than the unprocessed DSF. © 2014 Wiley Periodicals, Inc. and the American Pharmacists Association J Pharm Sci

Keywords: disulfiram; brain tumours; PLGA; implantable device; localised drug delivery; cancer; biodegradable polymers; blood brain barrier; controlled delivery

INTRODUCTION

Glioblastoma multiforme (GBM) is the most common primary malignant brain tumour in adults with a very poor prognosis. Even after surgery, radiotherapy and chemotherapy, the overall survival rate for patients with GBM is 42.4% at 6 months, 17.7% at 12 months and 3.3% at 2 years.[1] The current treatment for GBM is surgical resection of accessible tumour, which is often limited if the tumour is located near to critical regions of the brain, followed by radiotherapy and adjuvant chemotherapy. However, this has not been very successful, with a standard course of radiotherapy, following surgical removal of the tumour, extending a patients' life from 6 to only 9 months, whereas an increased dose of radiation is not possible, because of undesirable side effects.[2,3]

Systemic delivery of chemotherapeutic drugs into the neurons and glial tissues of the brain is challenging because of the presence of the blood–brain barrier (BBB), which consists of tight junctions between the endothelial cells lining the cerebral capillaries.[4] The BBB is very selective and consequently only low-molecular-weight, electrically neutral, hydrophobic molecules are able to freely cross this barrier.[5–7] Many chemotherapeutic drugs, which tend to be large, ionically charged and hydrophilic, cannot cross the BBB from the bloodstream into the brain at levels needed for therapeutic effect, which means that an intolerably high systemic drug levels are required in order to achieve the therapeutic levels required in the brain.[3,6,8,9] Furthermore, if the drug does manage to diffuse across the BBB, it can very quickly diffuse back making it difficult to obtain a constant therapeutic concentration after systemic administration. One option to overcome this issue is the use of implantable devices to deliver the chemotherapeutic drug directly to the tumour, which offers a number of advantages over systemic administration, including increased drug stability as it remains in the delivery device until released, direct delivery to the site of action, lower dose of drug required and reduced side effects because of the avoidance of systemic circulation.[10] Furthermore, local drug delivery may be suitable for the treatment of GBM as approximately 80%–90% return within 2 cm of the resection site.[3]

The Gliadel® wafer is an example of one such device, which was approved by the Food and Drug Administration in 1996 for the treatment of recurring GBM.[11,12] It is a disc-shaped, 200 mg biodegradable wafer 14 mm in diameter and 1 mm thick manufactured using a copolymer 1,3-bis-(p-carboxyphenoxy) propane and sebacic acid (in a molar ratio of 80:20) containing 3.85% (w/w) of the chemotherapeutic agent Carmustine.[9,10] The polymer and active ingredient are dissolved in dichloromethane, before they are spray dried into microspheres varying from 1 to 20 μm, which are then compressed into wafers. Following the surgical removal of a primary brain tumour, up to

Correspondence to: Christopher McConville (Telephone: +44-1902-322615; Fax: +44-1902-322714; E-mail: C.Mcconville@wlv.ac.uk)

Journal of Pharmaceutical Sciences

eight wafers are implanted in the resection cavity and the Carmustine is released from the wafers over a 5-day period, whereas the polymer matrix degrades over a period of 6–8 weeks.[11] Gliadel® wafers enable the delivery of a chemotherapeutic agent directly into the resection cavity and thus overcome the issues associated with BBB. A small randomised, double-blind, placebo-controlled clinical trial involving 32 patients demonstrated that the Gliadel® wafer increased the median survival rate, after surgery, for patients with grade IV tumours from 39.9 weeks to 58.1 weeks.[12] A much larger trial involving 240 participants demonstrated that the Gliadel® wafer (in addition to surgery and radiation) increased the median survival rate of patients with newly diagnosed high-grade gliomas from 11.6 months (placebo) to 13.9 months (Gliadel®).[13] A randomised placebo-controlled clinical trial in 222 patients with recurrent malignant gliomas demonstrated that Gliadel® increased the survival rate 23 weeks to 31 weeks, whereas the 6-month survival rate was 50% greater in those patients treated with Glidael® compared with the placebo group.[14] However, a Cochrane Review stated that Gliadel® results in a prolongation of survival without an increased incidence of adverse events when used as primary therapy, whereas in recurrent disease, it does not appear to confer any added benefit.[15] In addition, only a third of patients suffering from GBM respond to treatment with Carmustine,[16] whereas in some patients, cerebral oedema was reported as one of the major adverse effects associated with Gliadel®.[17] Other types of implantable devices, such as millirods,[18,19] disks/wafers,[20,21] foams[22] and gels[23] as well a range of micro and nanoparticle formulations[24–29] are currently being developed for the localised delivery of chemotherapeutic drugs to the brain.

Poly(lactic-co-glycolic acid) (PLGA) is a biodegradable and biocompatible copolymer that has been used in the manufacture of a range of drug delivery devices such as disc/wafers, rods, scaffolds, films, foams micro and nanoparticles to deliver a range of drugs from peptides and proteins to chemotherapeutic and analgesic drugs as well as antibiotics and vaccines in a sustained and controlled manner.[22,30–40] The drug release from a PLGA drug delivery device can be controlled by the ratio of lactic and glycolic acid in the polymer, the molecular weight of the PLGA used as well as the physiochemical properties of the active and the shape of the drug delivery device.[31,41–44] Furthermore, blending the PLGA with another polymer can influence the mechanical properties as well as the drug release properties of the device.[45]

Disulfiram (DSF), which is an antialcoholic drug, has been shown to have an anticancer effect against GBM,[46–48] which is copper (Cu) dependent[49,50] as Cu plays a crucial role in redox reactions and triggers the generation of reactive oxygen species (ROS) which induce apoptosis in human cells.[51] DSF can chelate Cu(II) forming a DSF/Cu complex which improves the transport of Cu into cancer cells and is a much stronger ROS inducer than Cu alone.[52,53] Drug-induced ROS accumulation is usually counterbalanced by the activation of NFκB, an antiapoptotic factor inhibiting ROS and ROS-induced cytotoxicity.[54] However, DSF is also capable of inhibiting activity of NFκB.[55] Furthermore, it has been demonstrated that DSF can potentiate the cytotoxic effect of other anticancer drugs and ionising radiation. These characteristics and its low toxicity make DSF an attractive candidate for the treatment of GBM.

MATERIALS AND METHODS

Materials

Poly(D,L-lactide-co-glycolide) with a 50:50 lactide–glycolide ratio and varying degradation rates ranging from days (DLG 1A), weeks (DLG 4A) to months (DLG 4E) were purchased from Evonik Industries (Birmingham, Alaska). DSF, dichloromethane copper (II) chloride ($CuCl_2$) and sodium dodecyl sulphate (SDS) were purchased from Sigma–Aldrich (Dorset, England) and all materials were used as supplied. The brain cancer cell line U373 was purchased from ATCC (Middlesex, UK).

Manufacture of 10% and 20% (w/w) DSF-Loaded PLGA Wafers Using the Direct Compression Method

The required amount of DSF and each PLGA were weighed out and then mixed together using a mortar and pestle. Four-hundred milligram of each DSF/PLGA blend was weighed out and placed into a 14-mm diameter die of a KBr press and compressed under 15 tonnes of pressure to produce either a 400-mg 10% or 20% (w/w) DSF-loaded PLGA wafer 1 mm thick and 14 mm in diameter.

Manufacture of 10 and 20% (w/w) DSF-Loaded PLGA Wafers Using the Solvent Casting Methods

The required amount of DSF and each PLGA were weighed out, then mixed together and dissolved in 50 mL of Dichloromethane (DCM) using a mortar and pestle. The DSF/PLGA solutions were then poured into a petri dish left for 2 weeks to allow the DCM to evaporate off leaving either a 10% or 20% (w/w) DSF-loaded PLGA disc. To ensure no residual solvent remained, the disc was placed into a vacuum oven for 3 days. Individual wafers (1 mm thick and 14 mm in diameter) weighing approximately 400 mg were subsequently cut out from the larger disc.

Manufacture of 10% and 20% (w/w) DSF-Loaded PLGA Wafers Using the Heat Compression Method

The required amount of DSF and each PLGA were weighed out and then mixed together using a mortar and pestle and subsequently placed onto a class plate heated to 80°C and allowed to soften for 2 min. The DSF/PLGA blend was compressed under 0.5 tonne of pressure to form a large DSF/PLGA disc 1 mm thick. Individual wafers (1 mm thick and 14 mm in diameter) weighing approximately 400 mg were subsequently cut out from the larger disc.

Content Uniformity and Drug Stability of 10% and 20% (w/w) DSF-Loaded PLGA Wafers

Each DSF-loaded PLGA wafer ($n = 4$) was cut into small pieces placed into 50 mL of DCM and left over night until completely dissolved. The DCM was subsequently evaporated offer and the DSF/PLGA residue was resuspended in 40 mL of ethanol causing the PLGA to precipitate out while the DSF remained in solution. The sample was then placed into an orbital shaking incubator (Unitron HT infors) at 37°C and 60 rpm overnight to ensure all of the DSF went into solution. The ethanol was then analysed using the DSF stability indicating HPLC method.

 DOI 10.1002/jps.24304

Determination of the Physical State of DSF in the PLGA Wafers

Thermal analysis of DSF, PLGAs and DSF-loaded PLGA wafers was conducted using a Q200 TA Instruments differential scanning calorimeter (DSC). Approximately 10 mg of each sample were added to a DSC pan and placed in the thermal chamber of the DSC. The DSC analysis was performed between 30°C and 90°C at a heating rate of 10°C/min. Control samples were prepared by mixing 9 mg of PLGA polymer and 1 mg of DSF (corresponding to a 10%, w/w, DSF loading) and subsequently analysed by DSC.

Morphological Evaluation of the 10% and 20% (w/w) DSF-Loaded PLGA Wafers

Scanning electron microscopy (SEM) images of the 10% (w/w) DSF-loaded PLGA wafers where taken using a Zeiss EVO50-EP scanning electron microscope. The samples were prepared by sticking the whole wafer to an aluminium stub using an adhesive carbon tab and then sputter coating them with gold.

Powder X-Ray Diffraction

The powder X-ray diffraction (PXRD) analysis was performed on DSF, PLGA and 10% (w/w) DSF-loaded PLGA wafers using a Panalytical Empyrean diffractometer (PANanalyical, Almelo, The Netherlands) with Cu Kα radiation ($\lambda = 1.54060$) at 40 kV and 40 mA between 5° and 80° (2θ) at 25°C. The DSF and PLGA powder samples were analysed as is, whereas the 10% (w/w) DSF-loaded PLGA wafers were ground into powder before being analysed.

In Vitro Release of the 10% and 20% (w/w) DSF-Loaded PLGA Wafers

Each DSF-loaded PLGA wafer ($n = 4$) was placed into a sealed flask containing 50 mL of 2% SDS and placed into an orbital shaking incubator (Unitron HT infors) at 37°C and 60 rpm. A 5-mL sample was taken and replaced with fresh media each day (except weekends) for the first 14 days, then on a Monday and a Friday for the last 2 weeks. The samples where filtered using a 0.45-μm filter and analysed using the DSF stability indicating HPLC method.

DSF HPLC Methodology

HPLC analysis was performed on an Agilent 1200 series HPLC (Agilent, Santa Clara, CA) with a Phenomenex Luna C18 4.6 × 150 mm^2 column with a 5-μM particle size (Phenomenex, Torrance, CA). The mobile phase comprises 80% HPLC grade methanol and 20% HPLC grade water. The flow rate was 1.00 mL/min, whereas UV detection was performed at a wavelength of 275 nm with an injection volume of 10 μL.

Cytotoxic Testing of the DSF Within the DSF-Loaded PLGA Wafers

One millilitre of the final content and drug stability solutions [section *Content Uniformity and Drug Stability of 10% and 20% (w/w) DSF-Loaded PLGA Wafers*] from the 10% (w/w) DSF-loaded PLGA wafers was diluted with 9 mL of sterile phosphate-buffered saline (PBS) solution to produce solutions with a DSF concentration of 0.1 mg/mL. A DSF control solution was produced by dissolving 40 mg of DSF in 50 mL of DCM and subsequently evaporating it off. The residual DSF was dissolved in 40 mL of ethanol and 1 mL of this solution was diluted with 9 mL of PBS solution.

The U373 brain cancer cell line was cultured in Dulbecco's modified Eagle medium (Lonza, Wokingham, UK) supplemented with 10% FCS, 2 mM L-glutamine, 50 units/mL penicillin, 50 μg/mL streptomycin. For *in vitro* cytotoxicity assay, the cells (5000 per well) were cultured in 96-well flat-bottomed microtiter plates overnight and exposed to 125 μm of the DSF samples and control as well as $CuCl_2$ (10 μM) for 72 h when a standard MTT assay[56] was performed on the cells and their percent vitality determined.

Statistical Analysis

Statistical analysis was performed using a one-way analysis of variance (ANOVA) (GraphPad Prism version 5.02 for Windows; GraphPad Software, San Diego, California). Post-hoc comparisons of the means were performed using Tukey's honestly significance difference test. A significance level of $p < 0.05$ was accepted to denote significance in all cases.

RESULTS

Content Uniformity and Drug Stability of the 10% and 20% (w/w) DSF-Loaded Wafers

Figure 1 demonstrates that all of the compressed (a) and heat compressed (c) PLGA wafers had an actual DSF content very similar to their theoretical content ($p \geq 0.05$), whereas the HPLC analysis did not detect any known or unknown degradation products of DSF (data not shown). This demonstrates that both the compression and heat compression manufacturing methods can be used to produce PLGA wafers containing stable DSF at the correct level. In the case of the solvent-casted PLGA wafers (b), the actual DSF content was significantly lower than the theoretical content ($p < 0.05$). However, the HPLC analysis did not detect any known or unknown degradation products of DSF, which would suggest that the DSF may have interacted with the PLGA as a result of the solvent casting process and was thus unable to be completely extracted from the wafer. This issue may limit the use of solvent casting as a manufacturing process for producing DSF-loaded PLGA wafers. Furthermore, the DSF precipitated out of the PLGA polymer DLG 1A upon removal of the DCM and accumulated in a number of areas on the surface of the large disc. Therefore, this polymer was no longer investigated using the solvent casting method.

Characterisation of the 10% and 20% (w/w) DSF-Loaded Wafers

Powder X-ray Diffraction

Powder X-ray diffraction studies were undertaken to confirm the crystalline characteristics of DSF within the wafers. Figure 2 shows the PXRD patterns for the PLGA polymers, DSF and the DSF-loaded wafers. The PLGA and DSF controls (Fig. 1a) demonstrate that the DSF control has a number of sharp high-intensity diffraction peaks, the full length of its PXRD pattern, which would suggest that it is highly crystalline, while the PLGA controls have a smooth halo PXRD pattern, which suggests that they are amorphous. The PXRD patterns for the compressed DSF-loaded wafers (Figs. 1b and 1c) are very similar to the pattern for the DSF control, with sharp high-intensity diffraction peaks, the full length of the pattern. This demonstrates that the DSF within the compressed DSF-loaded wafers is in its crystalline form, which would be expected as

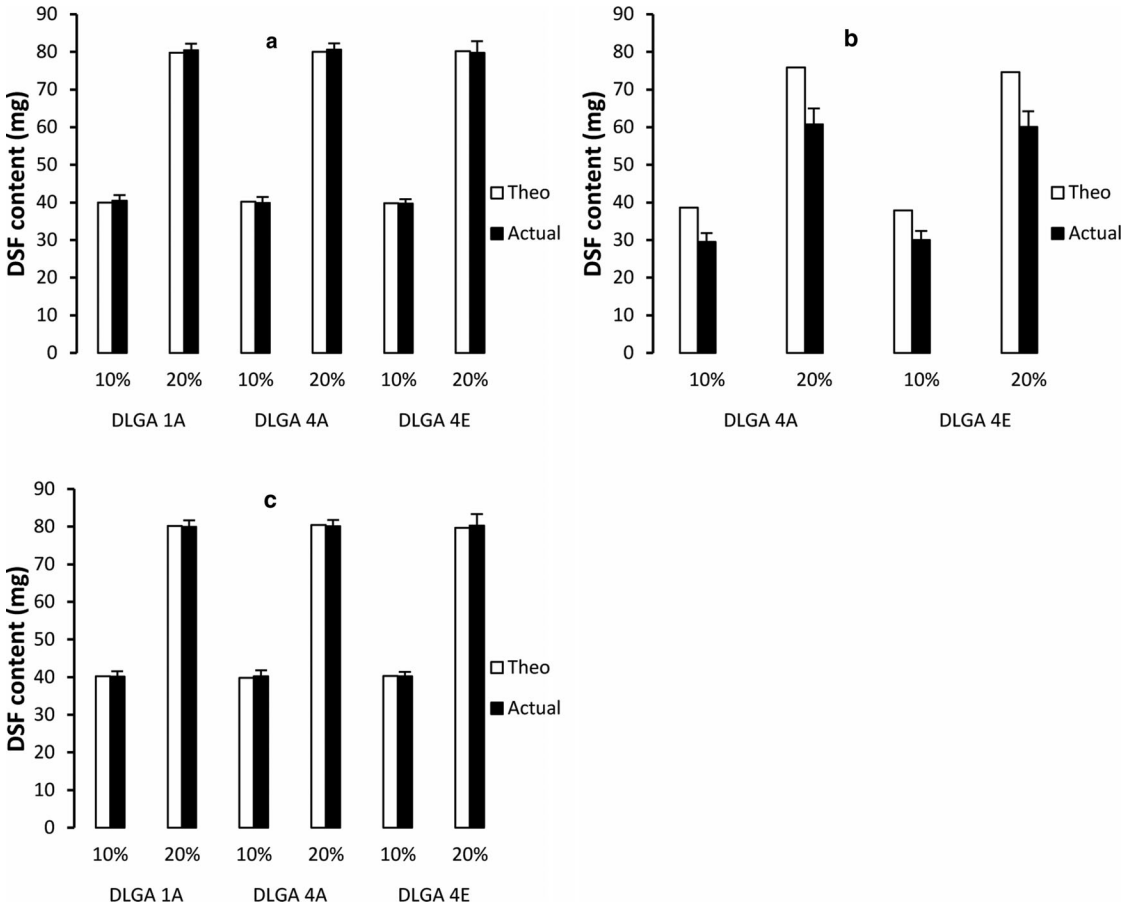

Figure 1. Theoretical and actual DSF content of the 10% and 20% DSF-loaded PLGA wafers manufactured using compression (a), solvent casting (b) and heat compression moulding (c).

the DSF and PLGA were simply blended together and then compressed into a disc. Therefore, we would not expect this process to have any influence on the physical state of the DSF within the wafer. The DSF-loaded wafers manufactured by solvent casting (Figs. 1d and 1e) have a halo PXRD pattern, similar to the PLGA controls, with sharp, low-intensity diffraction peaks, similar to the DSF control. This demonstrates that the DSF within the solvent-casted wafers has lost some of its crystalline structure as a result of it being dissolved within the PLGA polymers, which can be attributed to the DSF being dissolved in the DCM during the solvent casting process and the ability of the PLGA polymers to maintain the DSF in the dissolved state upon removal of the DCM.[57–59] The PXRD patterns for the DSF-loaded wafers manufactured by heat compression moulding where very similar to those of the PLGA controls, with a smooth halo pattern and no diffraction peaks associated with DSF. This would suggest that the DSF is dispersed at the molecular level and its crystallinity completely removed. The reason for this is that the wafers where manufactured at 80°C, which is above the melting temperature of DSF, consequently melting the DSF into its amorphous form and the subsequent cooling causes the polymer to solidify holding the DSF in its amorphous form.

Differential Scanning Calorimetry

The physicochemical state of DSF in the PLGA wafers was analysed using DSC (Fig. 3). The thermograms for the DSF-loaded wafers manufactured by compression have two distinct endothermic peaks (Figs. 3a and 3b). The sharp endothermic peak at approximately 71°C in all six wafer formulations is caused by the DSF, which has a melting point of approximately 70°C, whereas the much broader endothermic peak between 39°c and 55°C (depending on the type of polymer used to produce the wafers) corresponds to PLGA polymer, which has a glass transition temperature of approximately 45°C.[60] This demonstrates that the DSF in the compressed wafers is in its crystalline form, which corresponds to the PXRD data. Table 1 contains the melting enthalpies for the DSF-loaded wafers and the controls. Comparing the DSF melting enthalpies of the controls and the compressed DSF-loaded wafers shows that the DSF within the wafers had between 98.5% and 101.0% crystallinity.

The thermograms for the solvent-casted DSF-loaded wafers (Figs. 3c and 3d) have a single peak broad endothermic peak between 50°C and 70°C. The PXRD data show that the DSF in the solvent-casted wafers has a low level of crystallinity and thus we would expect to see an endothermic peak at approximately 70°C corresponding to melting enthalpy of the DSF. Furthermore, the broad peak associated with the polymer has shifted to the right by approximately 11°C–15°C. The lack of a DSF peak and the fact that the PLGA peak has moved to the right would suggest that there has been an interaction between the PLGA polymer and the DSF as a result of the solvent-casting process. This is corroborated by the melting enthalpies

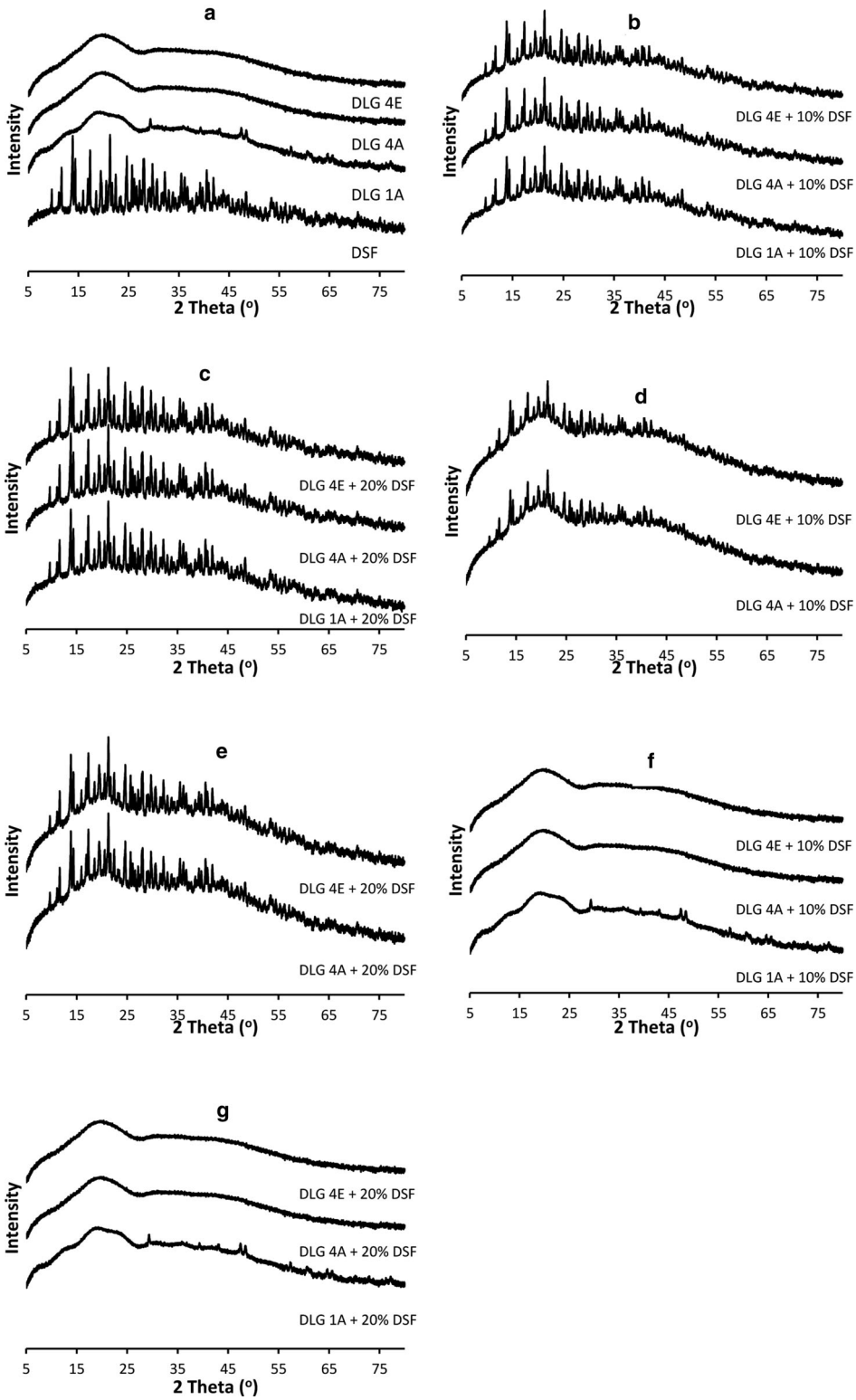

Figure 2. X-ray diffraction patterns for the DSF and PLGA controls (a), the 10% and 20% DSF-loaded wafers manufactured by compression (b and c), solvent casting (d and e) and heat compression moulding (f and g).

in Table 1, which demonstrate that the melting enthalpies of the broad peak in the wafers compared with the broad peak in the controls is between 26.0% and 39.5% greater. This extra energy is because of the DSF in the wafers, which would suggest that the DSF peak has shifted left because of an interaction between it and the PLGA polymers and is being masked by the broader polymer peak.

Figures 3e and 3f show the thermograms for the heat-compressed DSF-loaded wafers. The thermograms have no endothermic peak associated with the DSF, which would suggest

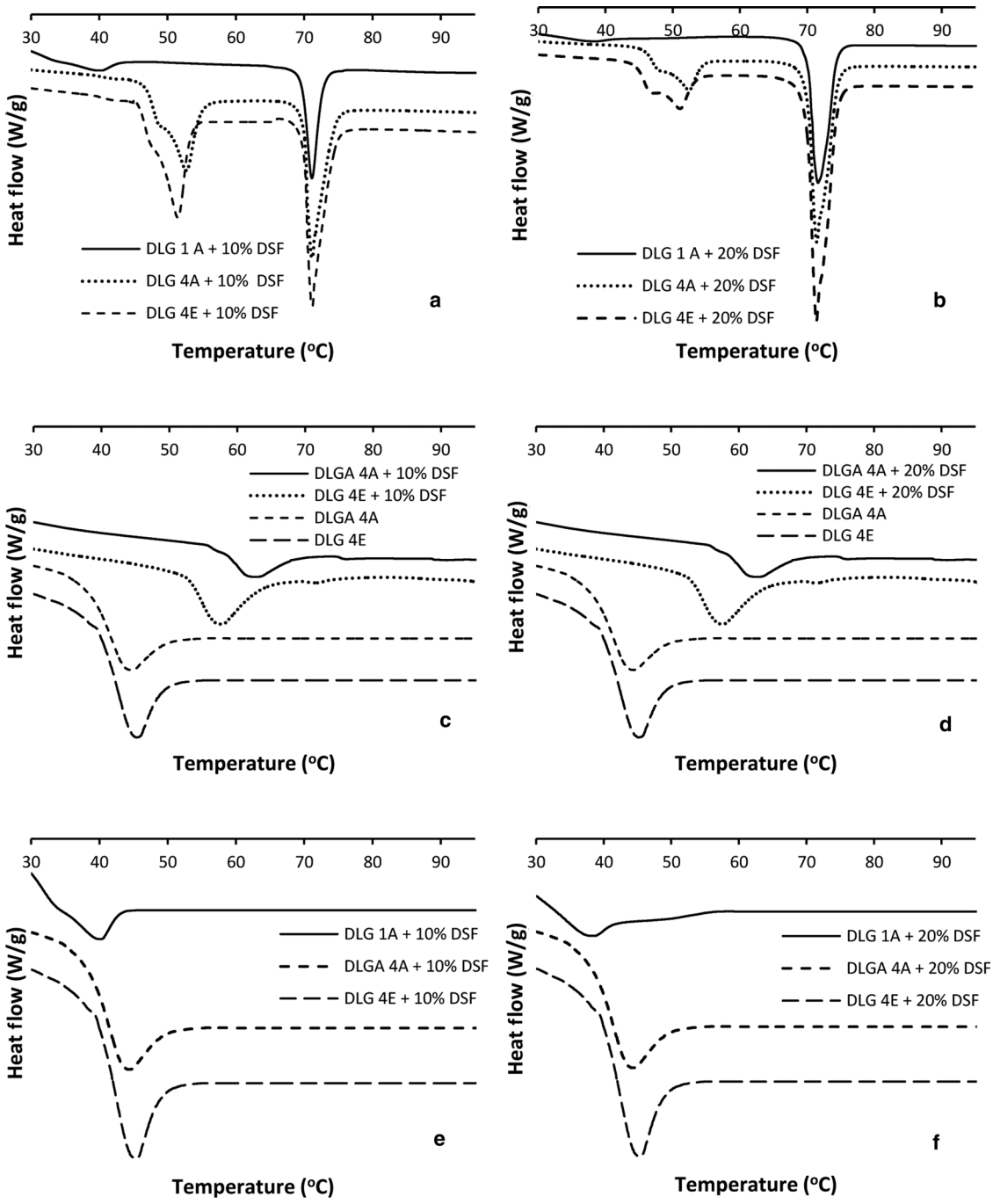

Figure 3. Differential scanning calorimeter thermograms for the 10% and 20% DSF-loaded wafers manufactured by compression (a and b), solvent casting (c and d) and heat compression moulding (e and f).

Table 1. The Enthalpy Values for the Polymer and DSF in both the 10% and 20% DSF-loaded wafers

	Controls			Compressed						Solvent Cast				Compression Moulded					
Peak	DLG 1A	DLG 4A	DLG 4E	DLG 1A		DLG 4A		DLG 4E		DLG 4A		DLG 4E		DLG 1A		DLG 4A		DLG 4E	
DSF loading				10%	20%	10%	20%	10%	20%	10%	20%	10%	20%	10%	20%	10%	20%	10%	20%
Polymer	1.8	7.3	7.6	1.8	1.6	7.2	6.5	7.7	6.7	9.2	10.1	9.5	10.6	1.8	1.5	7.4	6.6	7.6	6.5
DSF	9.8	9.9	9.8	9.7	19.6	9.9	19.5	9.7	19.8	N/A	N/A	N/A	N/A	0	0	0	0	0	0

 DOI 10.1002/jps.24304

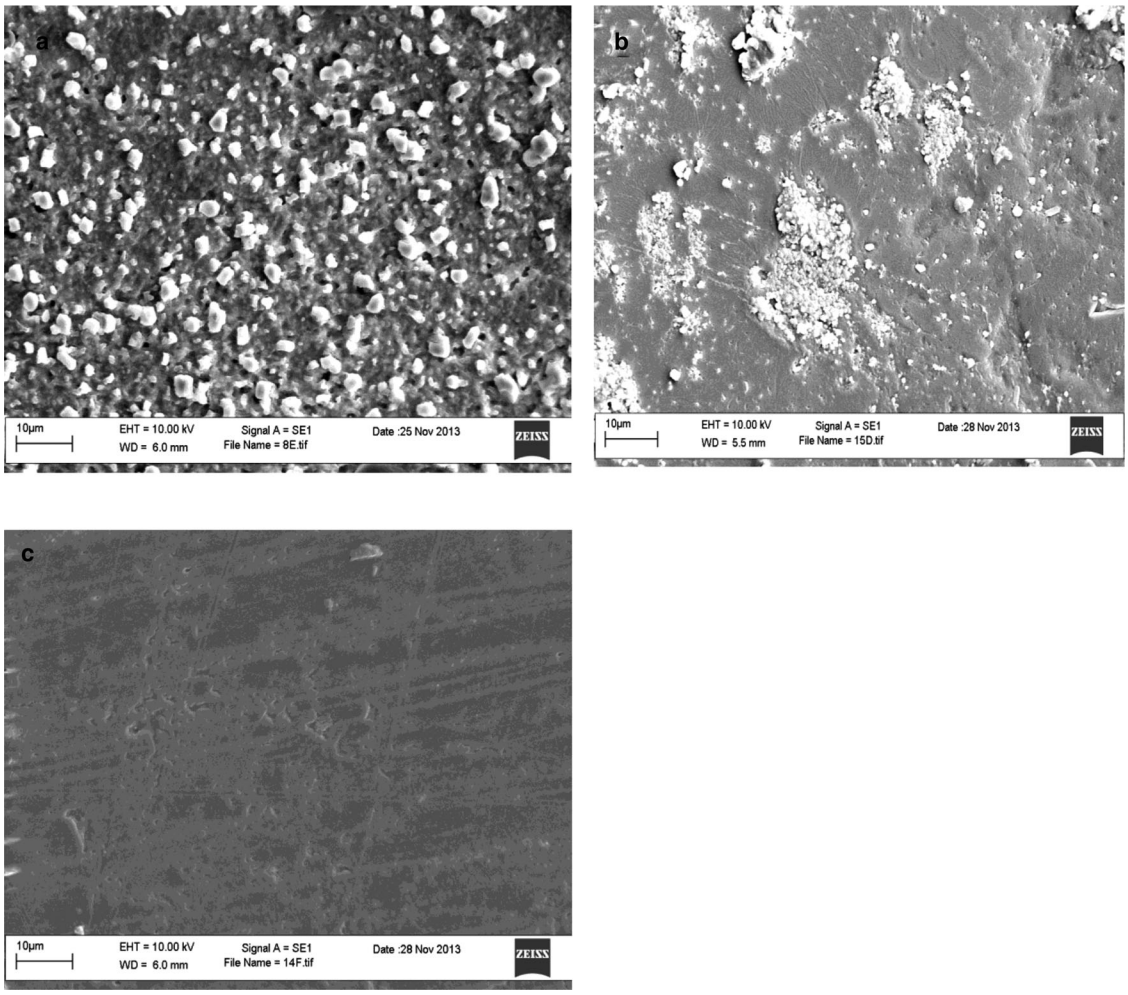

Figure 4. Representative SEM images of the DSF-loaded wafers manufactured by compression (a), solvent casting (b) and heat compression moulding (c).

that the DSF in the wafers is present in either and amorphous, dissolved or molecularly dispersed state and corroborates the PXRD data in Figures 1d and 1e.

Scanning Electron Microscopy

The surface morphology of the DSF-loaded PLGA wafers was analysed using SEM and representative SEM images are presented in Figure 4. The SEM images show that the compressed DSF-loaded wafers (Fig. 4a) have a large number of DSF particles on the surface, whereas the solvent-casted wafers (Fig. 4b) also have DSF particles on the surface, but at a lower level than the compressed wafers. The SEM images for the heat-compressed DSF-loaded wafers show that they have no DSF particles on their surface. The SEM images further corroborate the PXRD and DSC data, which suggest that the DSF in the compressed wafers is in its crystalline form, whereas the solvent-casted wafers contain a significantly lower amount of crystalline DSF and the heat compressed wafers contain no crystalline DSF.

In Vitro Release of DSF from the PLGA Wafers

In vitro release of DSF from PLGA wafers into 2% SDS over 28 days is presented in Figure 5. With the 10% (w/w) DSF-loaded compressed wafers, a day 1 burst is only observed for the DLG 1A PLGA polymer ($p < 0.05$), whereas both the DLGA 1A and 4 wafers with a 20% (w/w) DSF loading have a day 1 burst ($p < 0.05$). This observation was unexpected as the SEM images for the compressed wafers (Fig. 4a) clearly show a significant level of DSF particles on the surface of the wafer, therefore as it is these particles which contribute to the day 1 burst we would have expected all of the compressed wafers to show this trend. However, as the "burst effect" was only observed with the fastest degrading polymer (DLG 1A) for the 10% (w/w) DSF loading (Fig. 5a) and the fastest and second fastest degrading polymer (DLG 4A) for the 20% (w/w) DSF loading (Fig. 5b). We believe that in this case the trend is dependent on the degradation rate of the polymer and the DSF loading, with the 10% (w/w) DSF loading not being high enough to allow the DLG 4A polymer to have a significant day 1 burst. After day 1, the rest of the release is dependent on the degradation rate of the polymer for both the 10% and 20% (w/w) DSF loadings (Figs. 5a and 5b). Both DLG 1A and 4A wafers exhibited the tri-phasic release profile, which is commonly reported in many PLGA formulations,[61–63] where there is slow diffusion controlled-release between day 4 and 8 depending on the polymer, with approximately 12%–25% of the drug being released, followed by a dramatic increase in the release rate controlled by

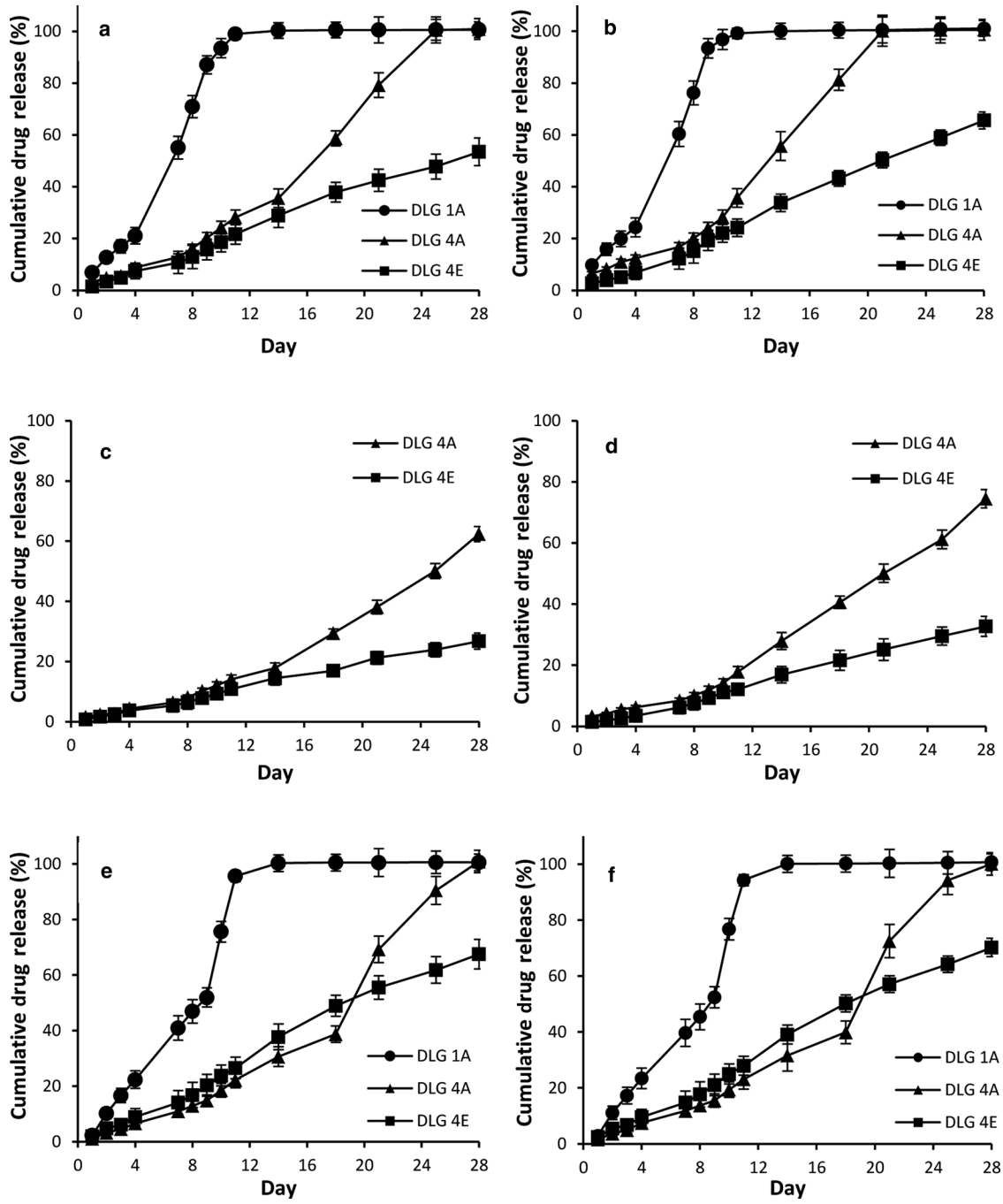

Figure 5. *In vitro* drug release for the 10% and 20% DSF-loaded wafers manufactured by compression (a and b), solvent casting (c and d) and heat compression moulding (e and f).

the degradation of the polymers and a subsequent slower drug release phase because of the exhaustion of the DSF within the wafer. The DLG 1A polymer, which had a degradation time of days, had released 100% of its DSF content by day 14 for both the 10% and 20% loading, whereas the DLG 4A polymer, which had a degradation rate of weeks, required until day 25 for the 10% loading and day 21 for the 20% loading. The initial phase of slow diffusion controlled release is because of the fact that the polymers have not yet started to degrade. However, by day 4 for the DLG 1A polymer and day 8 for the DLG 4A polymer, the second phase of drug release begins and continues at a much faster rate than the first phase. This second phase is a result of the polymers starting to degrade making the polymer more porous, allowing more release media to diffuse in and more dug to diffuse out. In contrast, the DLG 4E wafers maintained a slow, diffusion controlled-release profile for the entire 28 days, with approximately 54% and 65% of their DSF loading being released for the 10% and 20% loadings, respectively ($p < 0.05$). The reason for this release profile is because of the fact that this polymer takes 1–2 months to start degrading and therefore acted like a nondegradable polymer for the 28 days of release.

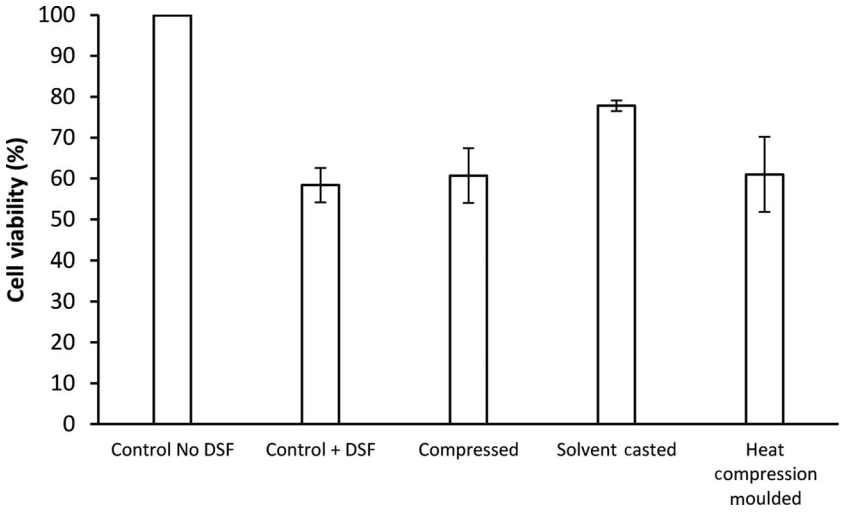

Figure 6. Cytotoxicity testing of the DSF extracted from the 10% (w/w) DSF-loaded wafers.

In the case of the solvent-casted wafers (Fig. 5c and 5d), only the DLG 4A and DLG 4E polymers were evaluated for their release. The release from these wafers is significantly lower compared with the wafers manufactured by compression ($p < 0.05$). The DLG 4A polymer has a bi-phasic release profile with slow, diffusion-controlled release until day 8, releasing approximately 8% of DSF with a 10% loading and 10% of DSF with a 20% loading. After day 8, the release rate begins to increase because of the degradation of the polymer, with the 10% DSF-loaded wafers releasing approximately 62% of their DSF content, whereas the 20% DSF-loaded wafers released approximately 75%. Like the wafers manufactured by compression, the solvent-cased DLG 4E wafers maintained a slow, diffusion-controlled release profile for the entire 28 days, with approximately 27% and 33% of their DSF loading being released for the 10% and 20% loadings, respectively ($p < 0.05$). We believe that the reason for the lower release of DSF from the solvent-casted wafers is because of the manufacturing process and the fact that most of the drug was either dissolved or dispersed within the polymer, which reduced the amount of drug on the surface of the polymer as evidenced by the SEM image (Fig. 4b). The less drug particles on the surface results in less pores being formed when these particle dissolve, which in turn reduces the diffusion of the release media into the wafers and the diffusion of DSF out of the wafers, subsequently slowing down the overall release rate. Furthermore, we also believe that the interaction between the DSF and the PLGA, as demonstrated by DSC (Figs. 3e and 3f), reduces the amount of DSF available for release (Fig. 1b), subsequently reducing its overall release rate.

The heat-compressed DSF-loaded wafers had no significant day 1 burst (Figs. 5e and 5f). This is because of the fact that the majority of the DSF is either dissolved or dispersed within the polymer, as evident by the DSC (Figs. 3e and 3f) and the PXRD (Figs. 2f and 2g) data, as well as the lack of DSF particles on the surface of the wafer (Fig. 4c). The release profiles for both the 10% and 20% loading DLG 1A and DLG 4A wafers exhibit the tri-phasic release profile similar to that seen with the compressed wafers. However, the slow diffusion controlled-release phase is extended out until either day 9 or 18 depending on the polymer, with approximately 39%–52% of their DSF content being released. The diffusion controlled-release phase was followed by an increase in the release rate controlled by the degradation of the polymers with the DLG 1A releasing 100% of its DSF content by day 14 and the DLG 4A by day 28. The DLG 4E heat-compressed wafers, such as the compressed wafers, had a diffusion controlled-release profile for the entire 28 days, with approximately 68% and 70% of their DSF content being released for the 10% and 20% loadings, respectively ($p < 0.05$). This release rate is significantly ($p < 0.05$) greater than that of the compressed wafers and is because of the DSF being dissolved or dispersed in the polymer, increasing both its diffusion rate through the polymer and its solubility in the release media.

This data demonstrate that the DSF release from the PLGA wafers can be controlled by the choice of polymer, drug loading and the manufacturing technique used to produce the wafers.

Cytotoxicity of the DSF in the PLGA Wafers

In order for the wafers to be effective, the DSF which they release needs to maintain its cytotoxicity during the manufacturing process. Therefore, we extracted the DSF from the wafers and added a known concentration to GBM cells and compared this with an unprocessed DSF control (Fig. 6). Figure 6 demonstrates that the DSF extracted from both the compressed and heat-compressed wafers has a comparable cytotoxicity to the unprocessed DSF ($p \geq 0.05$). This would suggest that the manufacturing processes of compression and heat compression have no significant effect on the cytotoxicity of the DSF. In contrast, the cytotoxicity of the DSF extracted from the solvent-casted wafers was significantly lower than the unprocessed DSF. However, we do not believe that this is because of the DSF being degraded as the HPLC analysis did not show any known or unknown impurities. We believe that it is because of the interaction between the PLGA and the DSF, which results in less DSF being extracted from the wafers as demonstrated by the content study (Fig. 2a). Therefore, the extraction solutions added to the GBM cells had a lower concentration of DSF resulting in a lower cytotoxicity.

CONCLUSION

This paper investigates the effect of different manufacturing techniques on the content uniformity, stability, physical state, release and cytotoxicity of DSF in 10% and 20% (w/w) DSF-loaded wafers. The paper demonstrates that neither technique has an adverse effect on the stability of the DSF within the wafers. However, the solvent casting technique results in an interaction between the PLGA and the DSF. The DSF contained in the wafers manufactured using the compression and solvent casting techniques retained approximately 98% and 40% of its crystallinity, respectively, whereas the DSF in those wafers manufactured by the heat compression moulding technique was completely amorphous. The *in vitro* release of DSF from the wafers is dependent on the degradation of the PLGA, the manufacturing technique used and the DSF loading. The DSF in the compressed and heat-compression-moulded wafers had a similar cytotoxicity to the unprocessed DSF. However, the cytotoxicity of the DSF in the solvent-casted wafers was significantly lower than the unprocessed DSF. This was because of the interaction of the DSF with the PLGA, rather than its degradation, resulting in less DSF being extracted and thus the extraction solution had a lower cytotoxicity. We believe that if successfully tested in an *in vivo* model, these wafer formulations offer an alternative to the current GBM treatments available, whereas localised delivery to the brain will overcome the issues associated with the BBB, reduce the dose of drug needed to provide a therapeutic effect and minimise the systemic side effects associated with other chemotherapeutic delivery options.

ACKNOWLEDGMENT

The authors would like to acknowledge the Early Research Award Scheme (ERAS) from the University of Wolverhampton who provided some of the funding to help complete this research.

REFERENCES

1. Ohgaki H, Dessen P, Jourde B, Horstmann S, Nishikawa T, Di Patre PL, Burkhard C, Schüler D, Probst-Hensch NM, Maiorka PC, Baeza N, Pisani P, Yonekawa Y, Yasargil MG, Lütolf UM, Kleihues P. 2004. Genetic pathways to glioblastoma: A population-based study. Cancer Res 64:6892–6899.

2. Ong BYS, Ranganath SH, Lee LY, Lu F, Lee H, Sahinidis NV, Wang C. 2009. Paclitaxel delivery from PLGA foams for controlled release in post-surgical chemotherapy against glioblastoma multiforme. Biomaterials 30:3189–3196.

3. Wang PP, Frazier J, Brem H. 2002. Local drug delivery to the brain. Adv Drug Deliv Rev 54:987–1013.

4. Reese TS, Karnovsky MJ. 1967. Fine structural localization of a blood–brain barrier to exogenous peroxidase. J Cell Biol 34:207–217.

5. Seelig A, Gottschlich R, Devant RM. 1994. A method to determine the ability of drugs to diffuse through the blood-brain barrier. PNAS 91:68–72.

6. Abbott NJ, Romero IA. 1996. Transporting therapeutics across the blood–brain barrier. Mol Med Today 2:106–113.

7. Kemper EM, van Zandbergen AE, Cleypool C, Mos HA, Boogerd W, Beijnen JH, van Tellingen O. 2003. Increased penetration of paclitaxel into the brain by inhibition of P-glycoprotein. Clin Cancer Res 9:2849–2855.

8. Grieg NH. 1987. Optimizing drug delivery to brain tumors. Cancer Treat Rev 14:1–28.

9. Siepmann J, Siepmann F, Florence AT. 2006. Local controlled drug delivery to the brain: Mathematical modeling of the underlying mass transport mechanisms. Int J Pharm 314:101–119.

10. Wolinsky JB, Colson YL, Grinstaff MW. 2012. Local drug delivery strategies for cancer treatment: Gels, nanoparticles, polymeric films, rods, and wafers. J Con Rel 159:14–26.

11. Fleming AB, Saltzman WM. 2002. Pharmacokinetics of the carmustine implant. Clin Pharm 41:403–419.

12. Valtonen S, Timonen U, Toivanen P, Kalimo H, Kivipelto L, Heiskanen O, Unsgaard G, Kuurne T. 1997. Interstitial chemotherapy with carmustine-loaded polymers for high-grade gliomas: A randomized double-blind study. Neurosurgery 41:44–48.

13. Westphal M, Hilt DC, Bortey E, Delavault P, Olivares R, Warnke PC, Whittle IR, Jaaskelainen J, Ram Z. 2003. A phase 3 trial of local chemotherapy with biodegradable carmustine (BCNU) wafers (Gliadel wafers) in patients with primary malignant glioma. Neuro Oncol 5:79–88.

14. Brem H, Piantadosi S, Burger PC. 1995. Placebo-controlled trial of safety and efficacy of intraoperative controlled delivery by biodegradable polymers of chemotherapy for recurrence. Lancet 345:1008–1012.

15. Hart MG, Grant R, Garside R, Rogers G, Somerville M, Stein K. 2011. Chemotherapeutic wafers for high grade Glioma. Cochrane Database Syst Rev 16:CD007294.

16. Brem H, Gabikian P. 2001. Biodegradable polymer implants to treat brain tumors. J Control Release 74:63–67.

17. Weber EL, Goebel EA. 2005. Cerebral edema associated with Gliadel wafers: Two case studies. Neuro Oncol 7:84–89.

18. Qian F, Szymanski A, Gao J. 2001. Fabrication and characterization of controlled release poly(D,L-lactide-co-glycolide) millirods. J Biomed Mater Res 55:512–522.

19. Weinberg BD, Blanco E, Gao J. 2008. Polymer implants for intratumoral drug delivery and cancer therapy. J Pharm Sci 97:1681–1702.

20. Ranganath SH, Wang C. 2008. Biodegradable microfiber implants delivering paclitaxel for post-surgical chemotherapy against malignant glioma. Biomaterials 29:2996–3003.

21. Sheleg SV, Korotkevich EA, Zhavrid EA, Muravskaya GV, Smeyanovich AF, Shanko YG, Yurkshtovich TL, Bychkovsky PB, Belyaev SA. 2002. Local chemotherapy with cisplatin-depot for glioblastoma multiforme. J Neurooncol 60:53–59.

22. Ong BYS, Ranganath SH, Lee LY, Lu F, Lee H, Sahinidis NV, Wang C. 2009. Paclitaxel delivery from PLGA foams for controlled release in post-surgical chemotherapy against glioblastoma multiforme. Biomaterials 30:3189–3196.

23. Vukelja SJ, Anthony SP, Arseneau JC, Berman BS, Cunningham CC, Nemunaitis JJ, Samlowski WE, Fowers KD. 2007. Phase 1 study of escalating-dose OncoGel (ReGel/paclitaxel) depot injection, a controlled-release formulation of paclitaxel, for local management of superficial solid tumor lesions. Anticancer Drugs 18:283–289.

24. Reguera-Nuñez E, Roca C, Hardy E, de la Fuente M, Csaba N, Garcia-Fuentes M. 2014. Implantable controlled release devices for BMP-7 delivery and suppression of glioblastoma initiating cells. Biomaterials 35:2859–2867.

25. Menei P, Capelle L, Guyotat J, Fuentes S, Assaker R, Bataille B, François P, Dorwling-Carter D, Paquis P, Bauchet L, Parker F, Sabatier J, Faisant N, Benoit JP. 2005. Local and sustained delivery of 5-fluorouracil from biodegradable microspheres for the radiosensitization of malignant glioma: A randomized phase II trial. Neurosurgery 56:242–248.

26. Beduneau A, Saulnier P, Benoit JP. 2007. Active targeting of brain tumors using nanocarriers. Biomaterials 28:4947–4967.

27. Koo H, Huh MS, Sun IC, Yuk SH, Choi K, Kim K, Kwon IC. 2011. In vivo targeted delivery of nanoparticles for theranosis. Acc Chem Res 44:1018–1028.

28. Meyers JD, Doane T, Burda C, Basilion JP. 2013. Nanoparticles for imaging and treating brain cancer. Nanomedicine 8:123–143.

29. Wang AZ. 2012. Nanoparticle drug delivery: Focusing on the therapeutic cargo. Nanomedicine 7:1463–1465.
30. Sharma G, Italia JL, Sonaje K, Tikoo K, Ravi Kumar MNV. 2007. Biodegradable in situ gelling system for subcutaneous administration of ellagic acid and ellagic acid loaded nanoparticles: Evaluation of their antioxidant potential against cyclosporine induced nephrotoxicity in rats. J Control Release 118:27–37.
31. Klose D, Siepmann F, Elkharraz K, Siepmann J. 2008. PLGA-based drug delivery systems: Importance of the type of drug and device geometry. Int J Pharm 354:95–103.
32. Desai KGH, Olsen KF, Mallery SR, Stoner GD, Schwendeman SP. 2010. Formulation and in vitro–in vivo evaluation of black raspberry extract-loaded PLGA/PLA injectable millicylindrical implants for sustained delivery of chemopreventive anthocyanins. Pharm Res 27:628–642.
33. Dong WY, Körber M, Esguerra L, Bodmeier R. 2006. Stability of poly(d,l-lactideco-glycolide) and leuprolide acetate in in-situ forming drug delivery systems. J Control Release 115:158–167.
34. Xiong Y, Zeng YS, Zeng CG, Du BL, He LM, Quan DP, Zhang W, Wang JM, Wu JL, Li Y, Li J. 2009. Synaptic transmission of neural stem cells seeded in 3-dimensional PLGA scaffolds. Biomaterials 30:3711–3722.
35. Gu H, Song C, Long D, Mei L, Sun H. 2007. Controlled release of recombinant human nerve growth factor (rhNGF) from poly[(lactic acid)-co(glycolic acid)] microspheres for the treatment of neurodegenerative disorders. Polym Int 56:1272–1280.
36. D'Souza SS, Selmin F, Murty SB, Qiu W, Thanoo BC, DeLuca PP. 2004. Assessment of fertility in male rats after extended chemical castration with a GnRH antagonist. AAPS PharmSci 6:94–99.
37. Mo Y, Lim LY. 2005. Paclitaxel-loaded PLGA nanoparticles: Potentiation of anticancer activity by surface conjugation with wheat germ agglutinin. J Control Release 108:244–262.
38. Yen SY, Sung KC, Wang JJ, Hu OYP. 2001. Controlled release of nalbuphine propionate from biodegradable microspheres: In vitro and in vivo studies. Int J Pharm 220:91–99.
39. Patel P, Mundrargi RC, Babu VR, Jain D, Rangaswamy V, Aminabhavi TM. 2008. Microencapsulation of doxycycline into poly(lactide-co-glycolide) by spray drying technique: Effect of polymer molecular weight on process parameters. J Appl Polym Sci 108:4038–4046.
40. Cui C, Stevens VC, Schwendeman SP. 2007. Injectable polymer microspheres enhance immunogenicity of a contraceptive peptide vaccine. Vaccine 25:500–509.
41. Zolnik BS, Leary PE, Burgess DJ. 2006. Elevated temperature accelerated release testing of PLGA microspheres. J Con Rel 112:293–300.
42. Ratajczak-Emselme M, Estebe JP, Dollo G, Chevanne F, Bec D, Malinovsky JM, Ecoffey C, Corre PL. 2009. Epidural, intrathecal and plasma pharmacokinetics study of epidural ropivacaine in PLGA-microspheres in sheep model. Eur J Pharm Biopharm 72:54–61.
43. Nair LS, Laurencin CT. 2007. Biodegradable polymers as biomaterials. Prog Polym Sci 32:762–798.
44. Frank A, Rath SK, Venkatraman SS. 2007. Controlled release from bioerodible polymers: Effect of drug type and polymer composition. J Control Release 102:333–344.
45. Mc Conville C, Major I, Friend DR, Clark MR, Woolfson AD, Malcolm RK. 2012. Development of polylactide and polyethylene vinyl acetate blends for the manufacture of vaginal rings. J Biomed Mater Res Part B 100B:891–895.
46. Liu P, Brown S, Goktug T, T Channathodiyil P, Kannappan V, Hugnot JP, Guichet PO, Bian X, Armesilla AL, Darling JL, Wang W. 2012. Cytotoxic effect of disulfiram/copper on human glioblastoma cell lines and ALDH-positive cancer-stem-like cells. Br J Cancer 107:1488–1497.
47. Triscott J, Lee C, Hu K, Fotovati A, Berns R, Pambid M, Luk M, Kast RE, Kong E, Toyota E, Yip S, Toyota B, Dunn SE. 2012. Disulfiram, a drug widely used to control alcoholism, suppresses the self-renewal of glioblastoma and over-rides resistance to temozolomide. Oncotarget 3:1112–1123.
48. Hothi P, Martins TJ, Chen L, Deleyrolle L, Yoon JG, Reynolds B, Foltz G. 2012. High throughput chemical screens identify disulfiram as an inhibitor of human glioblastoma stem cells. Oncotarget 3:1124–1136.
49. Cen D, Gonzalez RI, Buckmeier JA, Kahlon RS, Tohidian NB, Meyskens FL. 2002. Disulfiram induces apoptosis in human melanoma cells: A redox-related process. Mol Cancer Ther 1:197–204.
50. Cen D, Brayton D, Shahandeh B, Meyskens FL, Farmer PJ. 2004. Disulfiram facilitates intracellular Cu uptake and induces apoptosis in human melanoma cells. J Med Chem 47:6914–6920.
51. Barceloux DG. 1999. Copper. J Toxicol Clin Toxicol 37:217–230.
52. Burkitt MJ, Bishop HS, Milne L, Tsang SY, Provan GJ, Nobel CS, Orrenius S, Slater AF. 1998. Dithiocarbamate toxicity toward thymocytes involves their copper-catalyzed conversion to thiuram disulfides, which oxidize glutathione in a redox cycle without the release of reactive oxygen species. Arch Biochem Biophys 353:73–84.
53. Nobel CI, Kimland M, Lind B, Orrenius S, Slater AF. 1995. Dithiocarbamates induce apoptosis in thymocytes by raising the intracellular level of redox-active copper. J Biol Chem 270:26202–26208.
54. Nakano H, Nakajima A, Sakon-Komazawa S, Piao JH, Xue X, Okumura K. 2006. Reactive oxygen species mediate crosstalk between NF-kappaB and JNK. Cell Death Differ 13:730–737.
55. Yip NC, Fombon IS, Liu P, Brown S, Kannappan V, Armesilla AL, Xu B, Cassidy J, Darling JL, Wang W. 2011. Disulfiram modulated ROS–MAPK and NFkB pathways and targeted breast cancer cells with cancer stem cell-like properties. Br J Cancer 104:1564–s1881574.
56. Plumb JA, Milroy R, Kaye SB. 1989. Effects of the pH dependence of 3-(4,5-dimethylthiazol-2-yl)-2,5-diphenyl-tetrazolium bromide-formazan absorption on chemosensitivity determined by a novel tetrazolium-based assay. Cancer Res 49:4435–4440.
57. Lee SJ, Chae GS, An TK, Khang G, Cho SH, Lee HB. 2003. Preparation of 5-fluorouracil-loaded poly (L-lactide-co-glycolide) wafer and evaluation of in vitro release behaviour. Macromol Res 11:183–188.
58. Saliba JB, Junior SA, Silva GR, Yoshida MI, Mansur AAP, Mansur HS. 2012. Characterization and in vitro release of cyclosporine-a from poly (d,l-lactide–co–glycolide implants obtained by solvent/extraction evaporation. Quim Nova 35:723–727.
59. Pattnaik S, Swain K, Mallick S, Lin Z. 2011. Effect of casting solvent on crystallinity of ondansetron in transdermal films. Int J Pharm 406:106–110.
60. Ranganath SH, Kee I, Krantz WB, Chow PK, Wang C. 2009. Hydrogel matrix entrapping PLGA-paclitaxel microspheres: Drug delivery with near zero-order release and implantability advantages for malignant brain tumour chemotherapy. Pharm Res 26:2101–2114.
61. Zolnik BS, Leary PE, Burgess DJ. 2006. Elevated temperature accelerated release testing of PLGA microspheres. J Con Rel 112:293–300.
62. Berchane NS, Carson KH, Rice-Ficht AC, Andrews MJ. 2007. Effect of mean diameter and polydispersity of PLG microspheres on drug release: Experiment and theory. Int J Pharm 337:118–126.
63. Xu Q, Czernuszka JT. 2008. Controlled release of amoxicillin from hydroxyapatite-coated poly(lactic-co-glycolic acid) microspheres. J Control Release Soc 127:146–153.